DC Characteristic Analysis of Three-Phase LC Filter- Uncontrollable Rectifier Using Circuit DQ Transformation

Xin Geng, Xi-jun Yang, Zhe-min Zhang, Hou-jun Tang, Liang-yu Bai

Key Laboratory of Control of Power Transmission and Transformation, Ministry of Education
(Department of Electrical Engineering, Shanghai Jiao Tong University), Shanghai 200240, China

Abstract: The three-phase uncontrollable rectifiers are still widely applied, at present, in kinds of household appliances, because of its low cost, simple structure and excellent applicability. There are no LC filters in some simplified schematics. Sometimes, filter inductors are connected between rectifiers and power grids. For some higher requirements the three-phase passive power factor correction techniques with input LC filter are used in getting a higher power factor, just as the high power inverter air conditioners. Since the three-phase LC filter uncontrollable rectifier circuit is a strong coupling nonlinear system, it is difficult to analyse, model and select the parameters of LC filters. In this paper, circuit DQ transformation method is adopted to analyse the circuit's working principle better. It can convert the nonlinear circuit into linear system, then propose the novel concepts of the equivalent switching function, the control angle and the overlapping angle of uncontrollable rectifier. From this way, it makes the system controllable and discovers the controllability in three-phase LC filter uncontrollable rectifier systems. Through the analysis of the system DC characteristics, the expressions of output voltage, active power, passive power and power factor are calculated, which are identical to those of other controlled rectifiers. The relationship between the control angle and the load resistance are obtained through the simulation analysis. Experimental results on the rated output power 7.5kW three-phase rectifying system has proven the above theoretical analysis and circuit DQ transformation method. It has also proven the proposed concepts, which is practical to analyze the performances of the uncontrollable rectifier systems.

Key words: Three-phase passive PFC, Uncontrollable rectifier, DQ transformation, Power factor correction, Input LC filter, Equivalent switching function

1. Introduction

With the continuous advancement of related technologies, AC-DC-AC inverter technology has made considerable progress and the inverter-motor drive system is widely used in most of our lives. As the limitation of the single-phase supply, at present, almost all of the electrical equipments are powered by three-phase supply, such as high power air-conditioners. Uncontrollable rectifier-electrolytic capacitor system is taken as AC-DC converters' pre-stage circuit, which is the nonlinear load to power grid, so there are a mass of reactive currents, low order and relatively high order harmonic currents, those lead to low input power factor and high THD, which are inconsistent with the harmonic current issue standard: IEC61000-3-2 and IEC61000-3-12.

The nonlinear harmonic can be roughly divided into three types: harmonic voltage, mixed harmonic and harmonic current. For the silicon-controlled rectifier, matrix PWM rectifier and the current source rectifier, because of the large inductance of smoothing reactor following the output DC side, they show harmonic current source characteristics on the grid side. The larger inductance applied, the more significant harmonic current source characteristics appeared. Therefore, we need to use the parallel compensation before the rectifier bridge.

For the three-phase uncontrollable rectifier and voltage source rectifier, because of the large filter capacitance following the output DC side, they show harmonic voltage source characteristics on the grid side. The larger capacitance applied, the more significant harmonic voltage source characteristics appeared, and the higher peak current generated. Therefore, we need to use the series compensation before the rectifier bridge [1-4].

For larger power three-phase uncontrollable rectifier, it's connected a LC filter following the DC output side. The role of the rector is smooth DC current. For non-infinite power supply system, when the inductance is insufficient, the harmonic characteristics are between harmonic voltage sources and harmonic current source.

There are many passive filter techniques applied in three-phase AC-DC-AC inverter supply[5-8]. The input LC filter is an example. Nevertheless, its parameters are difficult to select and the performance of rectifiers is not convenient to analyze, because the LC filter-rectifier circuit is a nonlinear time-varying system, which is complex to build mathematical model. It is necessary to simplify or eliminate the influence of the switching actions. The circuit DQ transformation is one of the applicable approaches. The non-linear switching system can be transformed into a linear system, not including power switches. [9-13] Though harmonic components are ignored, it is significant to analyze its performances by utilizing linear system analysis method. In this paper, sub-circuits of the uncontrollable rectifier system are transformed by DQ transformation first. After that the equivalent low frequency DQ model is obtained and the novel concepts of the equivalent switching function, the control angle and the overlapping angle of the uncontrollable rectifier are also proposed. On these bases , the theoritical analysis and the experimental verification are performed in the DC characteristics of the active power, the passive power and the power factor.

2. DQ transformation of subcircuits

The three-phase LC filter uncontrollable rectifier-electrolytic capacitor-resistor system is shown in Fig.1. The system is partitioned into six subcircuits. They are: 1 power supply circuit; 2 resistor of power grid and filter inductor circuit; 3 input filter inductor circuit; 4 input filter capacitor circuit; 5 rectifier circuit; 6 output filter circuit and resistance load. The procedure is first to transform each subcircuit and gain its circuit DQ transformation model. And then to reconnect each model in terms of former function and gain low-frequency equivalent circuit model.

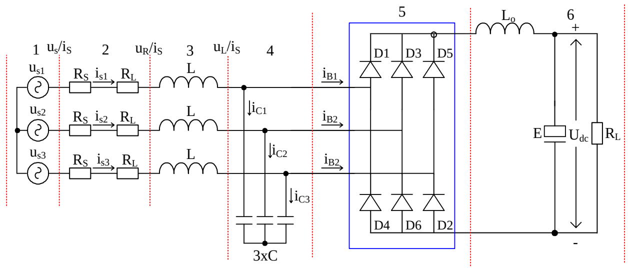

Fig.1 Three-phase LC filter uncontrollable rectifier-electrolytic capacitor-resistor load system and its subcircuit decompositions

We define the initial angle between q-axis in rotational coordinates and a-axis in stationary coordinates as φ, then the DQ transformation matrix is:

$$T=\sqrt{\frac{2}{3}}\begin{bmatrix}\cos(\omega t-\varphi) & \cos(\omega t-\alpha-\varphi) & \cos(\omega t+\alpha-\varphi)\\ \sin(\omega t-\varphi) & \sin(\omega t-\alpha-\varphi) & \sin(\omega t+\alpha-\varphi)\\ 1/\sqrt{2} & 1/\sqrt{2} & 1/\sqrt{2}\end{bmatrix} \quad (1)$$

$$T^{-1}=\sqrt{\frac{2}{3}}\begin{bmatrix}\cos(\omega t-\varphi) & \sin(\omega t-\varphi) & 1/\sqrt{2}\\ \cos(\omega t-\alpha-\varphi) & \sin(\omega t-\alpha-\varphi) & 1/\sqrt{2}\\ \cos(\omega t+\alpha-\varphi) & \sin(\omega t+\alpha-\varphi) & 1/\sqrt{2}\end{bmatrix} \quad (2)$$

Where, $-180^\circ \le \varphi \le 180^\circ$, φ represents input power factor angle, the displacement angle $\alpha = 2\pi/3$.

1) Power supply circuit

Without the loss of generality, suppose initial phase of the voltage source is zero, the input positive phase sequence voltages in stationary coordinates are:

$$u_s=\begin{bmatrix}u_{s1}\\ u_{s2}\\ u_{s3}\end{bmatrix}=U_{pm}\begin{bmatrix}\sin(\omega t)\\ \sin(\omega t-\alpha)\\ \sin(\omega t+\alpha)\end{bmatrix} \quad (3)$$

The transformation equation is equation (4) and the equivalent circuit is shown in Fig.2.

$$\begin{bmatrix}U_{qs}\\ U_{ds}\\ U_{0s}\end{bmatrix}=T\cdot u_s=\sqrt{\frac{3}{2}}U_{pm}\begin{bmatrix}\sin\varphi\\ \cos\varphi\\ 0\end{bmatrix} \quad (4)$$

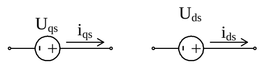

Fig.2 Power supply circuit

2) Resistor of power grid and filter inductor circuit

From fig.1, we can get equation (5).

$$u_R - u_s = (R_L + R_S) i_s \qquad (5)$$

After transformation, the resistor in DQ coordinates is described in (6) and the equivalent circuit is shown in Fig.3.

$$\begin{bmatrix} U_{qs} - U_{qR} \\ U_{ds} - U_{dR} \\ U_{0s} - U_{0R} \end{bmatrix} = T \cdot (u_R - u_s) = (R_L + R_S) T \cdot i_s$$

We define $\begin{bmatrix} I_{qs} \\ I_{ds} \\ I_0 \end{bmatrix} = T \cdot i_s$; then we can get equation (6) from equation (5).

$$\therefore \begin{bmatrix} U_{qs} - U_{qR} \\ U_{ds} - U_{dR} \\ U_{0s} - U_{0R} \end{bmatrix} = (R_L + R_S) \begin{bmatrix} I_{qs} \\ I_{ds} \\ I_0 \end{bmatrix} \qquad (6)$$

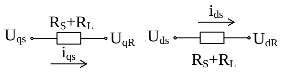

Fig.3 Resistor of power grid and filter inductor circuit

3) Input filter inductor circuit

From fig.1, we can get the equation (7).

$$L \frac{di_s}{dt} = u_R - u_L \qquad (7)$$

After transformation, the circuit in DQ coordinates is described in (8) and the equivalent circuit is shown in Fig.4.

$$\frac{d}{dt} \begin{bmatrix} i_{qs} \\ i_{ds} \end{bmatrix} = \frac{d}{dt}(T \cdot i_s) = \frac{dT}{dt} \cdot i_s + T \frac{d}{dt} i_s$$

$$\therefore \begin{bmatrix} U_{qR} \\ U_{dR} \\ U_{0R} \end{bmatrix} - \begin{bmatrix} U_{qL} \\ U_{dL} \\ U_{0L} \end{bmatrix} = T(u_R - u_L) = L \cdot T \cdot \frac{di_s}{dt}$$

$$= L \frac{d}{dt} \begin{bmatrix} i_{qs} \\ i_{ds} \\ i_{0s} \end{bmatrix} - L \frac{dT}{dt} \cdot i$$

$$= \omega_i L \begin{bmatrix} 0 & 1 & 0 \\ -1 & 0 & 0 \\ 0 & 0 & 0 \end{bmatrix} \begin{bmatrix} i_{qs} \\ i_{ds} \\ i_{0s} \end{bmatrix} + L \frac{d}{dt} \begin{bmatrix} i_{qs} \\ i_{ds} \\ i_{0s} \end{bmatrix}$$

The simplify equation is:

$$\begin{bmatrix} U_{qR} \\ U_{dR} \end{bmatrix} - \begin{bmatrix} U_{qL} \\ U_{dL} \end{bmatrix} = \omega_i L \begin{bmatrix} 0 & 1 \\ -1 & 0 \end{bmatrix} \begin{bmatrix} i_{qs} \\ i_{ds} \end{bmatrix} + L \frac{d}{dt} \begin{bmatrix} i_{qs} \\ i_{ds} \end{bmatrix} \qquad (8)$$

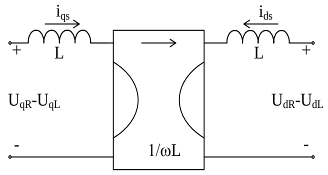

Fig.4 Input filter inductor circuit

4) Input filter capacitor circuit

From fig.1, the equation (9) can be gained.

$$\begin{bmatrix} i_{c1} \\ i_{c2} \\ i_{c3} \end{bmatrix} = C \frac{d}{dt} \begin{bmatrix} u_{L1} \\ u_{L2} \\ u_{L3} \end{bmatrix} \qquad (9)$$

After transformation, the circuit in DQ coordinates is described in figure (10) and the equivalent circuit is shown in Fig.5.

We define $\begin{bmatrix} i_{qc} \\ i_{dc} \\ i_{0c} \end{bmatrix} = T \begin{bmatrix} i_{c1} \\ i_{c2} \\ i_{c3} \end{bmatrix}$; then we can get from equation (9).

$$\begin{bmatrix} i_{qc} \\ i_{dc} \\ i_{0c} \end{bmatrix} = T \begin{bmatrix} i_{c1} \\ i_{c2} \\ i_{c3} \end{bmatrix} = CT \frac{d}{dt} u_L$$

$$= C \frac{d}{dt}(T u_L) - C \frac{dT}{dt} u_L$$

$$= C \frac{d}{dt} \begin{bmatrix} U_{qL} \\ U_{dL} \\ U_{0L} \end{bmatrix} + \begin{bmatrix} 0 & \omega_i C & 0 \\ -\omega_i C & 0 & 0 \\ 0 & 0 & 0 \end{bmatrix} \begin{bmatrix} U_{qL} \\ U_{dL} \\ U_{0L} \end{bmatrix}$$

The simplify equation is:

$$\begin{bmatrix} i_{qc} \\ i_{dc} \end{bmatrix} = \begin{bmatrix} 0 & \omega_i C \\ -\omega_i C & 0 \end{bmatrix} \begin{bmatrix} U_{qL} \\ U_{dL} \end{bmatrix} + C \frac{d}{dt} \begin{bmatrix} U_{qL} \\ U_{dL} \end{bmatrix} \qquad (10)$$

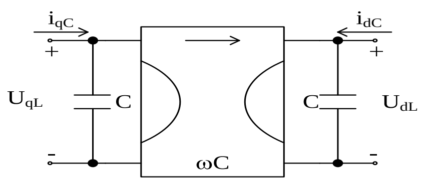

Fig.5 Input filter capacitor circuit

5) Rectifier circuit

First, we need to obtain each switching function of six power diodes in three-phase uncontrollable rectifier. Through simulations and experiments, it can be seen that as long as L, C was selected properly and there was a certain load, the conduction angle of each diode is 120°. The curves of switching function are shown in Fig. 6.

Where u_a, u_b and u_c represent input phase voltages, f_1~f_6 represent the switching function of D1~D6 respectively, the angle between f1 and phase voltage positive semi-cycle zero-crossing point is θ. $0 \le f_1 \sim f_6 \le 1$, $f_1+f_3+f_5=1$, $f_4+f_6+f_2=1$. We also know that θ is the function of load. When load is light, θ is relatively small, and vice versa. The range of θ is generally from 25° to 90°.

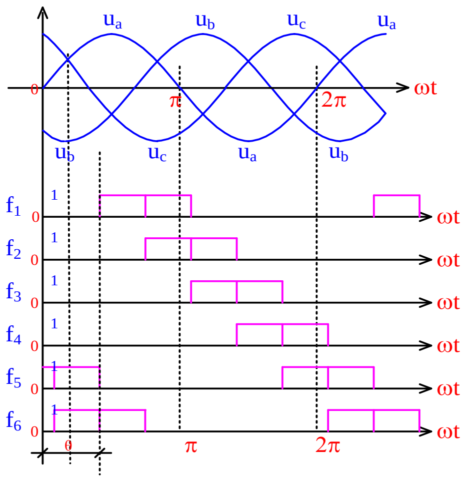

Fig.6 Mains phase voltage and equivalent switching function of power diode

We can get the Fourier expression of f_i, i=1, 2, 3, 4, 5, 6;

$$f_1=\frac{1}{3}+\frac{\sqrt{3}}{\pi}\sum_{n=0}\left\{\begin{array}{l}\frac{1}{3n+1}\sin\left[(3n+1)(\omega t-\theta+\frac{\pi}{6})-\frac{\pi}{2}n\right]\\+\frac{1}{3n+2}\sin\left[(3n+2)(\omega t-\theta+\frac{\pi}{6})-\frac{\pi}{2}n-\frac{\pi}{2}\right]\end{array}\right\}\quad(11)$$

$$f_2=\frac{1}{3}+\frac{\sqrt{3}}{\pi}\sum_{n=0}\left\{\begin{array}{l}\frac{1}{3n+1}\sin\left[(3n+1)(\omega t-\theta+\frac{\pi}{6})+\frac{\pi}{2}n-\frac{\pi}{3}\right]\\+\frac{1}{3n+2}\sin\left[(3n+2)(\omega t-\theta+\frac{\pi}{6})+\frac{\pi}{2}n+\frac{5\pi}{6}\right]\end{array}\right\}\quad(12)$$

$$f_3=\frac{1}{3}+\frac{\sqrt{3}}{\pi}\sum_{n=0}\left\{\begin{array}{l}\frac{1}{3n+1}\sin\left[(3n+1)(\omega t-\theta+\frac{\pi}{6})-\frac{\pi}{2}n-\frac{2\pi}{3}\right]\\+\frac{1}{3n+2}\sin\left[(3n+2)(\omega t-\theta+\frac{\pi}{6})-\frac{\pi}{2}n+\frac{\pi}{6}\right]\end{array}\right\}\quad(13)$$

$$f_4=\frac{1}{3}+\frac{\sqrt{3}}{\pi}\sum_{n=0}\left\{\begin{array}{l}\frac{1}{3n+1}\sin\left[(3n+1)(\omega t-\theta+\frac{\pi}{6})+\frac{\pi}{2}n-\pi\right]\\+\frac{1}{3n+2}\sin\left[(3n+2)(\omega t-\theta+\frac{\pi}{6})+\frac{\pi}{2}n-\frac{\pi}{2}\right]\end{array}\right\}\quad(14)$$

$$f_5=\frac{1}{3}+\frac{\sqrt{3}}{\pi}\sum_{n=0}\left\{\begin{array}{l}\frac{1}{3n+1}\sin\left[(3n+1)(\omega t-\theta+\frac{\pi}{6})-\frac{\pi}{2}n+\frac{2\pi}{3}\right]\\+\frac{1}{3n+2}\sin\left[(3n+2)(\omega t-\theta+\frac{\pi}{6})-\frac{\pi}{2}n+\frac{5\pi}{6}\right]\end{array}\right\}\quad(15)$$

$$f_6=\frac{1}{3}+\frac{\sqrt{3}}{\pi}\sum_{n=0}\left\{\begin{array}{l}\frac{1}{3n+1}\sin\left[(3n+1)(\omega t-\theta+\frac{\pi}{6})+\frac{\pi}{2}n+\frac{\pi}{3}\right]\\+\frac{1}{3n+2}\sin\left[(3n+2)(\omega t-\theta+\frac{\pi}{6})+\frac{\pi}{2}n+\frac{\pi}{6}\right]\end{array}\right\}\quad(16)$$

And then the equivalent switching action time on the midpoints of three bridge arms (u_{as} , u_{bs} and u_{cs}) in power switch matrix are

$$\left\{\begin{array}{l}f_1-f_4=\frac{2\sqrt{3}}{\pi}\sum_{n=0}\left\{\begin{array}{l}\frac{1}{3n+1}\sin\left[(3n+1)(\omega t-\theta+\frac{\pi}{6})\right]\cos\frac{\pi}{2}n\\-\frac{1}{3n+2}\sin\left[(3n+2)(\omega t-\theta+\frac{\pi}{6})\right]\sin\frac{\pi}{2}n\end{array}\right\}\\f_3-f_6=\frac{2\sqrt{3}}{\pi}\sum_{n=0}\left\{\begin{array}{l}\frac{1}{3n+1}\sin\left[(3n+1)(\omega t-\theta+\frac{\pi}{6})-\frac{2\pi}{3}\right]\cos\frac{\pi}{2}n\\-\frac{1}{3n+2}\sin\left[(3n+2)(\omega t-\theta+\frac{\pi}{6})+\frac{2\pi}{3}\right]\sin\frac{\pi}{2}n\end{array}\right\}\\f_5-f_2=\frac{2\sqrt{3}}{\pi}\sum_{n=0}\left\{\begin{array}{l}\frac{1}{3n+1}\sin\left[(3n+1)(\omega t-\theta+\frac{\pi}{6})+\frac{2\pi}{3}\right]\cos\frac{\pi}{2}n\\-\frac{1}{3n+2}\sin\left[(3n+2)(\omega t-\theta+\frac{\pi}{6})+\frac{4\pi}{3}\right]\sin\frac{\pi}{2}n\end{array}\right\}\end{array}\right.\quad(17)$$

According to the physical meaning of high-frequency synthesis method and switching function theorem, the output voltage of rectifier is calculated by equation (18) and the transformed circuit is shown in Fig.7.

$$\begin{array}{l}U_{dc}=\left[f_1-f_4\quad f_3-f_6\quad f_5-f_2\right]\begin{bmatrix}u_a'\\u_b'\\u_c'\end{bmatrix}\\=DT^{-1}\begin{bmatrix}U_{qL}\\U_{dL}\end{bmatrix}=\left[n_q\quad n_d\right]\begin{bmatrix}U_{qL}\\U_{dL}\end{bmatrix}\end{array}\quad(18)$$

Where,

$$\left\{\begin{array}{l}D=\left[f_1-f_4\quad f_3-f_6\quad f_5-f_2\right]\\\begin{bmatrix}n_q\\n_d\end{bmatrix}^T=\begin{bmatrix}\frac{3\sqrt{2}}{\pi}\sum_{n=0}\left\{\begin{array}{l}\frac{1}{3n+1}\sin\left[3n\omega t-(3n+1)(\theta-\frac{\pi}{6})+\varphi\right]\cos\frac{\pi}{2}n\\-\frac{1}{3n+2}\sin\left[3(n+1)\omega t-(3n+2)(\theta-\frac{\pi}{6})-\varphi\right]\sin\frac{\pi}{2}n\end{array}\right\}\\\frac{3\sqrt{2}}{\pi}\sum_{n=0}\left\{\begin{array}{l}\frac{1}{3n+1}\cos\left[3n\omega t-(3n+1)(\theta-\frac{\pi}{6})+\varphi\right]\cos\frac{\pi}{2}n\\+\frac{1}{3n+2}\cos\left[3(n+1)\omega t-(3n+2)(\theta-\frac{\pi}{6})-\varphi\right]\sin\frac{\pi}{2}n\end{array}\right\}\end{bmatrix}^T\end{array}\right.\quad(19)$$

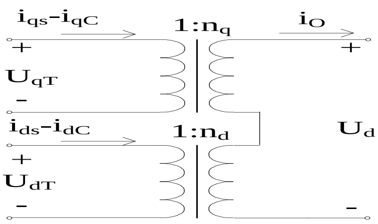

Fig.7 Rectifier circuit

6) Output filter circuit and resistance load

After transformation, the output voltage equation is equation (20) and the transformed circuit is in Fig.8.

$$U_{dc} = U_{\mathrm{d}} \tag{20}$$

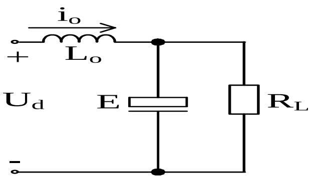

Fig.8 Output filter circuit and resistance load

Reconstruct the transformed sub-circuits in terms of former function and complete equivalent DQ circuit model of three-phase LC filter uncontrollable rectifier-electrolytic capacitor-resistor load system is obtained as shown in Fig.9.

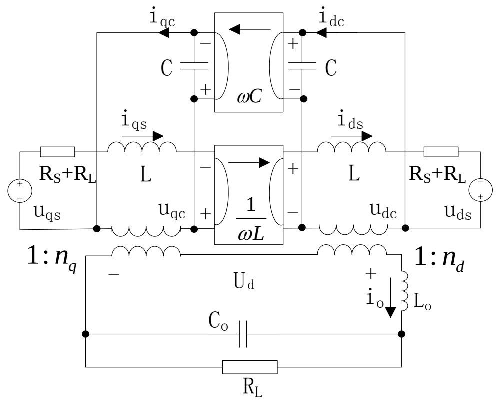

Fig.9 Circuit DQ model of LC filter uncontrollable rectifier system

3. DC characteristic analysis of LC filter uncontrollable rectifier system

To perform DC analysis, the DQ equivalent model in Fig.9 can be further simplified by shorting inductors and opening capacitors, the result is shown in Fig.10, which can be used to analyze various kinds of DC characteristic.

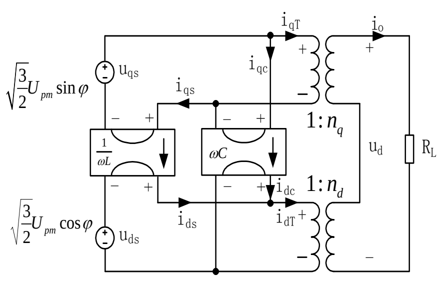

Fig.10 DC circuit of three-phase LC filter uncontrollable rectifier system

According to Fig.10, Kirchhoff voltage loop equations are (21) and gyrator equations are (22).

$$\begin{cases} U_{qs} = U_{qT} + U_{qL} \\ U_{ds} = U_{dT} - U_{dL} \\ i_{qs} = i_{qT} + i_{qc} \\ i_{ds} = i_{dT} - i_{dc} \\ \dfrac{i_{qT}}{n_q} = \dfrac{i_{dT}}{n_d} \\ U_{qT} n_q + U_{dT} n_d = U_d = \dfrac{i_{dT}}{n_d} R_L \end{cases} \tag{21}$$

$$\begin{cases} U_{qL} = \omega L i_{ds} \\ U_{dL} = \omega L i_{qs} \\ i_{qC} = \omega C U_{dT} \\ i_{dC} = \omega C U_{qT} \end{cases} \tag{22}$$

Then the expressions of output voltage, voltage gain, active power, passive power and power factor can be calculated respectively.

3.1 Output voltage

From (3) and (19), n_q, n_d, U_{qs} and U_{ds} are brought into the equation (18), the output voltage is expressing in equation (23)

$$U_d = \frac{3\sqrt{3}U_{pm}}{(1-\omega^2 LC)\pi} \sum_{n=0} \left\{ \begin{array}{l} \dfrac{1}{3n+1}\cos\left[3n\omega t - (3n+1)(\theta - \dfrac{\pi}{6})\right]\cos\dfrac{\pi}{2}n \\ -\dfrac{1}{3n+2}\cos\left[3(n+1)\omega t - (3n+2)(\theta - \dfrac{\pi}{6})\right]\sin\dfrac{\pi}{2}n \end{array} \right\} \tag{23}$$

From the above (23), it clearly indicates that DC voltage is the function of L, C and load resistor. The larger the product of LC is, the higher DC voltage is. As load is larger, θ becomes greater and DC voltage is lower. The maximum amplitude of voltage appears in the period of nearly no-load, at that time, only the product of LC influences DC voltage. It can be interpreted that, without load, input filters' LC parallel resonance reach the maximum amplitude, so the voltages before and after the bridge both reach the maximum amplitude. When load increases, non-linear loads is coupled to the front of rectifier as a complex non-linear impedance. Then parallel resonance between LC and resistor are produced, and the amplitude of DC voltage is decreasing, which may be even lower than that of the input line voltage. Where $3\sqrt{3}U_{pm}/\pi$ is no-load DC voltage (without electrolytic capacitor), i.e.

$$3\sqrt{3}U_{pm}/\pi = 3\sqrt{3}\cdot 220\sqrt{2}/\pi = 514.9\mathrm{V};$$

It has physical meaning. The value of $1/(1-\omega^2 LC)$ represents boost-multiple of the input filter parallel resonance, if the input filter inductor is 25mH and the input filter capacitor is

35μF, we can get $1/(1-\omega^2 LC) \approx 1.10$. It is identical to the simulation and experiment results. The value of $\sum_{n=0}\{\ \}$ reflects the variation degrees caused by load changing, it is in the range of [0, 1]. The larger the load is, the smaller the value of $\sum_{n=0}\{\ \}$ is. In this way, output voltage is fully decided by the above three factors.

Since the high-frequency harmonic content occupies a very small proportion, to simplification, six and in multiples of six order output voltage harmonic components are ignored. The output voltage is calculated by equation (24).

$$U_d = \frac{3\sqrt{3}U_{pm}}{(1-\omega^2 LC)\pi}\cos(\theta - \frac{\pi}{6}) \qquad (24)$$

Furthermore, output DC voltage gain G(i.e. the ratio of the output DC voltage to the amplitude of input phase voltage) is calculated by equation (25).

$$G = \frac{U_d}{U_{pm}} = \frac{3\sqrt{3}}{(1-\omega^2 LC)\pi}\cos(\theta - \frac{\pi}{6}) \qquad (25)$$

Where $\cos(\theta - \pi/6) \overset{\Delta}{=} \cos\theta'$ stands for load variation, θ is the angle between switching function of diode D1 and power grid phase voltage, θ' represents the control angle of diode and it is close to natural changing phase point with no-load.

Therefore, without considering the harmonic components, the expression completely explains the changing rules of the output voltage.

When the load is heavier or the inductor current is large, considering the longer diode reverse recovery time and the forward conductive voltage, the rectifier bridge currents will be overlapping and the conduction angle of diodes will be larger than 120°. At overlapping time, output DC voltage is the half of the sum of instantaneous value of the two changing phase voltages. It will lead to the distortion of the output voltage waveform and the decrease of the average value.

Suppose the overlapping angle is ϒ, and the output voltage is calculated by equation (26).

$$U_d = \frac{3\sqrt{3}U_{pm}}{(1-\omega^2 LC)\pi}\cos(\theta' + \frac{\gamma}{2})\cos\frac{\gamma}{2} \qquad (26)$$

The overlapping angle for the SCR is calculated by equation(27).

$$\gamma = \arccos(\cos\theta' - I_d / I_m) - \theta' \qquad (27)$$

It can be applied in LC filter-uncontrollable system, too. The I_d is the DC current and the I_m is the current amplitude in front of the rectifier. Since $\gamma > 0$, the larger γ is, the lower U_d is. Considering the inductor, the overlapping angle can be described as equation (28).

$$\cos\alpha - \cos(\alpha + \gamma) = 2I_d X_B / (\sqrt{6}U_2) \qquad (28)$$

The X_B stands for equivalent inductive reactance of transformer and filter inductor, the larger filter capacitor is, the smaller equivalent inductive reactance and overlapping angle are.

In addition, from the equation (23), we can also see another phenomenon. When $\omega^2 = \frac{1}{LC}$, the U_d will gain a very high voltage amplitude.

This phenomenon explains why the DC voltage can be higher times than the AC voltage amplitude in the applications of a Three-Phase LC Filter- Uncontrollable Rectifier.

So we can draw a conclusion, some special high harmonics can generate a very high DC voltage in the DC side of the Three-Phase LC Filter- Uncontrollable Rectifier when the voltage f AC side distortion, swells, sags and other cases.

In the same time, when the system starts to connect into the grid, we need avoid the special high harmonics, $\omega^2 = \frac{1}{LC}$, generating in the AC side. Therefore, the soft-switch may be necessary to apply.

3.2 Active power and passive power

To simplify the analysis, elided the harmonic components, the input current i_{qs} and i_{ds} are calculated by equation (29).

$$\begin{cases} i_{qs} = \dfrac{9\sqrt{6}U_{pm}\cos(\theta - \frac{\pi}{6})\sin(-\theta + \frac{\pi}{6} + \varphi)}{(1-\omega^2 LC)^2 \pi^2 R_L} \\ \quad + \sqrt{\dfrac{3}{2}}\dfrac{\omega C U_{pm}\cos\varphi}{1-\omega^2 LC} \\ i_{ds} = \dfrac{9\sqrt{6}U_{pm}\cos(\theta - \frac{\pi}{6})\cos(-\theta + \frac{\pi}{6} + \varphi)}{(1-\omega^2 LC)^2 \pi^2 R_L} \\ \quad - \sqrt{\dfrac{3}{2}}\dfrac{\omega C U_{pm}\sin\varphi}{1-\omega^2 LC} \end{cases} \qquad (29)$$

From (4) and (29), i_{qs}, i_{ds}, U_{qs} and U_{ds} are substituted, the active power P and passive power Q are calculated by equation (30)(31).

$$P = U_{qs}i_{qs} + U_{ds}i_{ds} = \frac{27U_{pm}^2\cos^2(\theta-\frac{\pi}{6})}{(1-\omega^2LC)^2\pi^2R_L} = S\cos(\theta-\frac{\pi}{6}) = S\cos\theta' \quad (30)$$

$$\begin{aligned} Q &= U_{qs}i_{ds} - U_{ds}i_{qs} = \frac{27U_{pm}^2\cos(\theta-\frac{\pi}{6})\sin(\theta-\frac{\pi}{6})}{(1-\omega^2LC)^2\pi^2R_L} - \frac{3\omega CU_{pm}^2}{2(1-\omega^2LC)} \\ &= P\tan(\theta-\frac{\pi}{6}) - \frac{3\omega CU_{pm}^2}{2(1-\omega^2LC)} = P\tan\theta' - \frac{3\omega CU_{pm}^2}{2(1-\omega^2LC)} \end{aligned} \quad (31)$$

The S is the apparent power and the active power P is the function of control angle θ', whose expression is identical to the three-phase linear circuit. According to the equation (31), the first term represents the variable passive power. When P is given, passive power at mains is in positive proportion to $\tan\theta'$. It means that regulation of passive power relies on active power regulation. The second term represents the passive power produced by input filter, and it is constant when the filtering parameters are decided. These expressions are similar to some rectifiers', such as matrix rectifier.

The relation of active power, passive power and apparent power are shown in Fig.11. As the increasing of θ, active power, passive power and apparent power are all monotone increasing. When the θ is smaller than 1.4 radian (80.22°), the active power increases linearly but the passive power increases nonlinearly. When the θ is greater than 1.4 radian, all of the powers increase rapidly in uncontrollable region. So when designing parameters, we need make sure the θ is less than 1.4 radian.

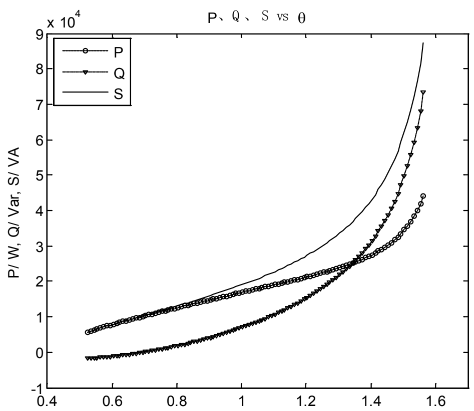

Fig.11 Relation of active power, passive power, apparent power VS θ

3.3 Input power factor

The input power factor PF is calculated by equation (32).

$$PF = \frac{P}{\sqrt{P^2+Q^2}} = \frac{\cos^2(\theta-\frac{\pi}{6})}{\sqrt{\cos^4(\theta-\frac{\pi}{6}) + \left[\frac{1}{2}\sin(2\theta-\frac{\pi}{3}) - \frac{1}{18}\pi^2R_L\omega C(1-\omega^2LC)\right]^2}} \quad (32)$$

It can be seen that PF is the function of input filtering parameters LC and θ, and the relation between the power factor and the θ is shown in Fig.12.

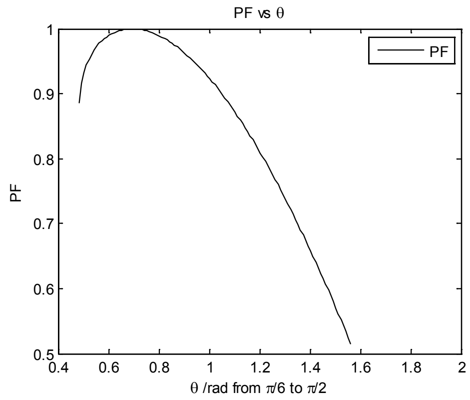

Fig.12 Relation of power factor VS θ

When the θ is equal to 0.7 radian (40.11°), it presents as a resistance. When the θ is smaller than 0.7 radian, it presents as a capacitance. When the θ is greater than 0.7 radian, it presents as a inductance.

3.4 Approximately unitary power factor operation

Only if the Q≈0, power factor is unitary approximately.

$$\begin{aligned} Q &= \frac{27U_{pm}^2\cos(\theta-\frac{\pi}{6})\sin(\theta-\frac{\pi}{6})}{(1-\omega^2LC)^2\pi^2R_L} - \frac{3\omega CU_{pm}^2}{2(1-\omega^2LC)} \\ &= P\tan(\theta-\frac{\pi}{6}) - \frac{3\omega CU_{pm}^2}{2(1-\omega^2LC)} \approx 0 \end{aligned} \quad (33)$$

Then:

$$\theta \approx \frac{1}{2}\arcsin\left[\frac{1}{9}(1-\omega^2LC)\omega C\pi^2R_L\right] + \frac{\pi}{6} \quad (34)$$

The solution of inverse sine function should be in the range of [90° , 180°]. Only if $R_L \le \frac{9}{(1-\omega^2LC)\omega C\pi^2} = 3.18k\Omega$, power factor can be unitary, it means the power factor is very low when the resistor is large or the load is light. In theory, the input power factor of LC filter-uncontrollable rectifier system is impossible to be exact one.

4. Simulation analysis and experimental verification

4.1 Simulation analysis

Fig.13 show a traditional Three-Phase LC Filter- Uncontrollable Rectifier circuit which applied in, at present, such as high power air-conditioners.

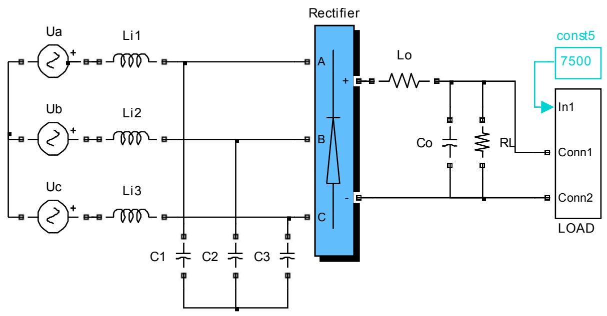

Fig.13 Traditional Three-Phase LC Filter- Uncontrollable Rectifier circuit

When the rated power is 7.5kW, the filter inductor is 25mH and the filtering capacitor is 35μF(Y connection), the waveforms of the mains phase voltage and current, the mains line voltage, the pre-bridge phase and the line voltage are shown in Fig.14(a). The average of the DC voltage is 549.1V. The mains phase current THD is close to zero, the displacement factor and the input power factor approach one.

In order to gain the control angle θ clearly, the amplitudes of main phase voltages are divided by ten. From Fig.14.(b), the control angle θ is 34.2°. By simulation, the active power is 7.599kW, the capacitance passive power is 0.6201kVar and the apparent power is 7.624kVA. According to the above expressions about the P, Q and S, the active power is 7.7944kW, the passive power is 1.1606kVar and the apparent power is 7.8803kVA.

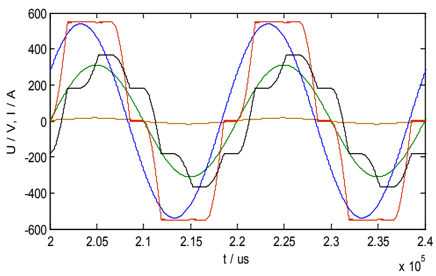

(a)

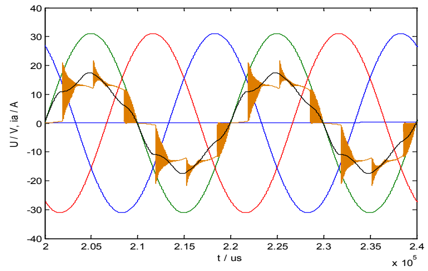

(b)

Fig.14 Simulation of three-phase LC filter - uncontrollable rectifier - electrolytic capacitor – resistor load system (a) Waveforms of voltages and currents (b) Waveforms of mains phase voltages, phase current and diode current

The simulation results are close to the calculated results. It clearly indicates that the theoretical analysis is correct.

Using the parameter-scanning method to find out the relationship between the load resistor and the control angle, the results are shown in table 1 and the curve is shown in Fig.15.

Table 1 In the different cases of output power

Load resistor $R_L(\Omega)$	Control angle θ (Rad)	Active power P(W)	Passive power Q (Var)	Apparent power S (kVA)	Power facto PF
15	57.6	4031x3	2660x3	23325x3	0.8347
20	49.5	3861x3	1537x3	17270x3	0.929
25	43.56	3514x3	796.8x3	12983x3	0.9752
30	39.6	3146x3	314.4x3	9996x3	0.995
35	39.6	2820x3	5.01x3	7952x3	1.00
40	34.2	2533x3	-206.7x3	6459x3	0.9966
45	32.4	2291x3	-350.8x3	5372x3	0.9885
50	31.5	2080x3	-454.4x3	4533x3	0.977
55	30.6	1910x3	-523.7x3	3922x3	0.9644
65	28.2	1632x3	-612.2x3	3038x3	0.9363
80	27.9	1335x3	-674.5x3	2237x3	0.8926
100	27.9	1075x3	-698.4x3	1643x3	0.8382
200	28.8	548.2x3	-668.1x3	747x3	0.6344
500	30.6	226.8x3	-658.9x3	486x3	0.3255
1000	34.2	121.3x3	-640.9x3	425x3	0.186

The fitting equation is $\theta = 69.16e^{-0.056R} + 27.19$. The control angle is the exponential function of load, and the range of θ is about from 25° to 120°. With light load or even no-load, the control angle changes a little. When the load is larger, the change rate of control angle becomes significantly faster.

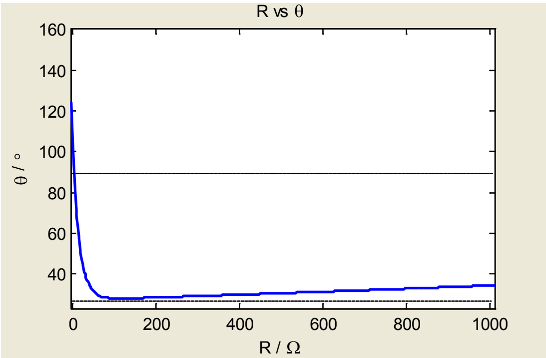

Fig.15 Relationship between load resistor and θ

4.2 Experimental verification

In order to verify the validity of the circuit DQ transformation model, the equivalent switching function and the control angle in three-phase LC filter-uncontrollable rectifier, my experiments are performed at rated power 7.5kW with a three-phase uncontrollable rectifier 35A/1200V, and the silicon steel inductor is 25mH and the CBB65 capacitor is 35uF/1200V. The circuit of experimental system is show in Fig.16.

The experimental results are identical to theoretical and simulation analysis, which are shown in table 2, table 3 and Fig.17.

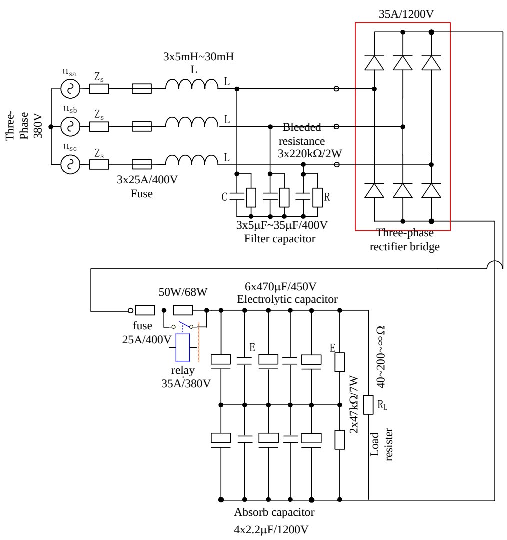

Fig.16 Experimental system

Table 2 Input and Output parameters (inductor 25mH/ capacitor 35uF Y connection)

Mains phase voltage (Vrms)	223.6	222.3	221.6
Mains current (Arms)	2.54	3.59	5.41
DC voltage(V)	601	570	563
Input Power factor	0	0.46	0.74
Input displacement factor	0	0.60	0.83
Current distortion rate	13.0	13.5	11.7
Output power (kW)	0	0.48 x3	1.00 x3
Control angle (°)	27.9	27.8	27.9

Table 3 Input and Output parameters (inductor 25mH/ capacitor 35uF Y connection)

Mains phase voltage (Vrms)	221.0	221.2	221.0
Mains current (Arms)	7.14	8.86	10.4
DC voltage(V)	555	543	531
Input Power factor	0.87	0.95	0.98
Input displacement factor	0.93	0.97	0.99
Current distortion rate	10.4	9.8	10.6
Output power (kW)	1.46 x3	1.19 x3	2.28 x3
Control angle (°)	31.8	39.6	41.2

The load determines the change of the control angle, and then the change of the control angle produces by the active power and the passive power's changing.

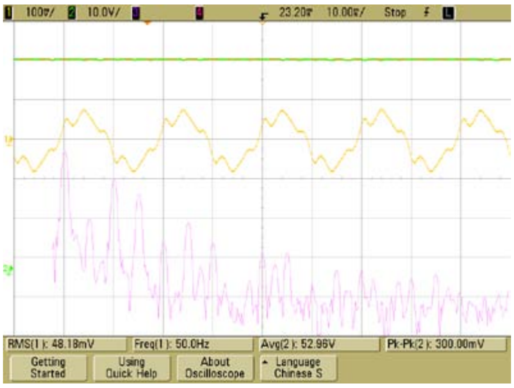

(a)

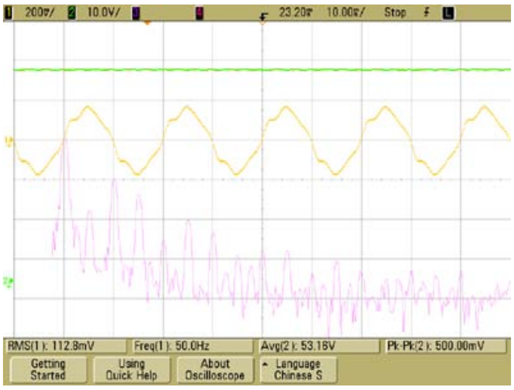

(b)

Fig.17 Input current and DC voltage waveform (a) In the case of light load (mains phase current is 4.818Arms) (b) In the case of heavy load (mains phase current is 11.28 Arms)

5. Conclusion

Although, the rectifier-electrolytic capacitor-resistor load system is not a high-frequency controllable system. It contains plenty of low-frequency harmonic current components. However, by using an appropriate LC filter, the low-frequency harmonic currents and the power distortion are greatly reduced. Using the circuit DQ transformation method can transform the system into a linear circuit, so the same approaches, which are applied in the controllable rectifier, can be used to analyze the rectifier-electrolytic capacitor- resistor load system, including some novel concepts as the equivalent switching function, the control angle and the overlapping angle etc. thus uncontrollable rectifiers has their controllability, too. The expressions of the output voltage, the active power, the passive power and the power factor are clear and easy to be understanded. At last, the simulations and experiments at a rated output power 7.5kW system has proved the correctness of the theoretical analysis.

Reference:

[1] Caliskan V, Perreault D J, Jahns T M, Kassakian J G. Analysis of three-phase rectifiers with constant-voltage loads [J]. IEEE Trans Circuits Syst, 2003, 50(9): 1220–1225.

[2] Peng F. Z. Harmonic sources and filtering approaches[J]. IEEE Trans on Industry Applications, 2001, 74, 7(4): 18-25.

[3] Lian K L, Perkins B K, Lehn P W. Harmonic Analysis of a Three-Phase Diode Bridge Rectifier Based on Sampled-Data Model[J]. Power Delivery, IEEE Transactions, 2008, 23(2): 1088-1096.

[4] Wagner V E, et al. Effects of harmonics on equipment[J]. IEEE Trans on PWRD, 1993, 8(2): 672-700.

[5] Li Xiaoqing, Chen Guozhu. An Approach to Harmonic Suppression Based on Triple Harmonics Injection with Passive Circuit [J]. *Automation of Electric Power Systems*, 2007, 31(14): 61-65.

[6] Pejovic P, Janda Z. A novel harmonic-free three-phase diode bridge rectifier applying current injection [C]. *Proceedings of the 1999 Fourteenth Annual Applied Power Electronics Conference and Exposition*, Mar 14-18, 1999, Dallas, TX, USA. Piscataway, NJ, USA, IEEE, 1999: 241-247.

[7] ZHOU Luo-wei, LUO Quan-ming. Dc And Ac Analysis of Three-Phase Three-Switch Boost Type SMR Based On DQ Transformation [J]. *Proceedings of the CSEE*, 2002, 22(7): 71-75.

[8] Chun T. Rim, Dong Y. Hu, Gyu H. Cho. Graphical D-Q transformation of general power switching converters [C]. *Industry Applications Society Annual Meeting, Conference Record of the 1988 IEEE 2-7 Oct*. 1988: 940 - 945.

[9] CAI Wen, YANG Xi-jun, GONG You-min. Research on Power Characteristics of Matrix Rectifier [J]. *Automation of Electric Power Systems*, 2006, 30(8): 27-31.

[10] ZHOU Hui, BAO Zhi-hua. Research on Matrix Converter Using dq Transformation Journal of Suzhou University (Natural Sciences), 1997, 13(3): 79-85.

[11] RIMS C T, HU D Y, CHO G H. Transformers as Equivalent Circuit for Switches: General Proofs and Q-D Transformation-based Analyses [J]. *IEEE Trans on Industry Applications*, 1990, 26(4):

777-785.

[12] Soo-Bin Han, Nam-Sup Choi, Chun-Taik Rim, Gyu-Hyeong Cho. Modeling and analysis of static and dynamic characteristics for buck-type three-phase PWM rectifier by circuit DQ transformation [J]. *Power Electronics, IEEE Transactions*, March 1998, 13(2): 323-336.

[13] Soo-Bin Han, Nam-Sup Choi, Chun-Taik Rim, Gyu-Hyeong Cho. Modeling and analysis of buck type three phase PWM rectifier by circuit DQ transformation [C]. *Power Electronics Specialists Conference, 1995. PESC '95 Record, 26th Annual IEEE*, 18-22 June 1995: 431-43